C. R. Palevol 18 (2019) 599–617

Contents lists available at ScienceDirect

Comptes Rendus Palevol

www.sciencedirect.com

General Palaeontology, Systematics, and Evolution (Vertebrate Palaeontology)

The first skull of *Anthropornis grandis* (Aves, Sphenisciformes) associated with postcranial elements

Le premier crâne d'itAnthropornis grandis (Aves, Sphenisciformes) associé à des éléments postcrâniens

Carolina Acosta Hospitaleche[a,b,*], Nadia Haidr[b,c], Ariana Paulina-Carabajal[b,d], Marcelo Reguero[a,b,e]

[a] *División Paleontología Vertebrados, Museo de La Plata, Universidad Nacional de La Plata, Paseo del Bosque s/n., B1900FWA La Plata, Argentina*
[b] *Consejo Nacional de Investigaciones Científicas y Técnicas (CONICET), C1425FQB Buenos Aires, Argentina*
[c] *Unidad Ejecutora Lillo (FML-CONICET), Calle Miguel Lillo 205, T4000 San Miguel de Tucumán, Argentina*
[d] *Instituto de Investigaciones en Biodiversidad y Medioambiente (INIBIOMA), CONICET-Universidad Nacional del Comahue, Quintral 1250 (8400), San Carlos de Bariloche, Argentina*
[e] *Instituto Antártico Argentino, 25 De Mayo 1143, San Martín, 1650 Buenos Aires, Argentina*

ARTICLE INFO

Article history:
Received 4 January 2019
Accepted after revision 18 June 2019
Available online 30 August 2019

Handled by Michel Laurin

Keywords:
Fossil penguin
Anatomy
Paleoneurology
Paleobiology
Submeseta Formation
Eocene
Antarctica

ABSTRACT

Associated penguin remains found in Bartonian levels of the Submeseta Formation (Seymour Island, Antarctica), including cranium and mandible, both partial tarsometatarsi, and some other fragmentary bones, are analyzed here. This specimen preserves the first cranium reliably assigned to the giant form *Anthropornis grandis*, and constitutes the first opportunity to taxonomically assign a cranial material to any of the Antarctic penguin species. A discussion of the diet preferences and feeding mechanisms of *A. grandis* is supported here by three-dimensional paleoneurological and cranial-jaw muscular reconstructions. We propose that *A. grandis* was a penguin with a voluminous musculature strongly attached to the neck and skull, adapted to chase and hunt fish during diving.

© 2019 Académie des sciences. Published by Elsevier Masson SAS. All rights reserved.

Mots clés :
Manchot fossile
Anatomie
Paléoneurologie
Paléobiologie

RÉSUMÉ

Les restes associés aux manchots trouvés dans les niveaux de Bartonien dans la formation de Submeseta (île Seymour, Antarctique), y compris le crâne et la mandibule, des tarsométatarses partiels et quelques autres os fragmentaires, sont analysés ici. Ce spécimen conserve le premier crâne attribué de manière fiable à la forme géante *Anthropornis grandis* et constitue la première occasion d'affecter de manière taxonomique un matériau crânien

* Corresponding author. División Paleontología Vertebrados, Museo de La Plata, Universidad Nacional de La Plata, Paseo del Bosque s/n., B1900FWA La Plata, Argentina.
E-mail addresses: acostacaro@fcnym.unlp.edu.ar (C. Acosta Hospitaleche), nadiahaidr@gmail.com (N. Haidr), premjisaurus@yahoo.com.ar (A. Paulina-Carabajal), mreguero@dna.gov.ar (M. Reguero).

https://doi.org/10.1016/j.crpv.2019.06.003
1631-0683/© 2019 Académie des sciences. Published by Elsevier Masson SAS. All rights reserved.

Formation de Submeseta
Éocène
Antarctique

à l'une des espèces de manchots antarctiques. Une discussion sur les préférences alimentaires et les mécanismes d'alimentation d'*A. grandis* est étayée ici par des reconstructions paléoneurologiques en trois dimensions et une reconstruction musculaire crâne–mâchoire. Nous proposons qu'*A. grandis* était un manchot à la musculature volumineuse, fortement attachée au cou et au crâne, adapté à la poursuite et à la chasse des poissons en plongée.

© 2019 Académie des sciences. Publié par Elsevier Masson SAS. Tous droits réservés.

1. Introduction

Anthropornis Wiman, 1905 is a genus described more than a century ago and one of the most remarkable Eocene penguins found in Antarctica. The robustness and massiveness of its postcranial bones caught the attention of Carl Wiman in 1905, and made it worthy of the name *Anthropornis*, meaning "man-bird" (Wiman, 1905a). For many years, *Anthropornis* was considered the largest penguin ever, until giant isolated tarsometatarsi of *Palaeeudyptes klekowskii* were discovered in the Eocene of Antarctica (Acosta Hospitaleche, 2014). Regardless of size, *Anthropornis* remained an intriguing taxon because, except for the tarsometatarsus, other skeletal elements were barely known (Jadwiszczak, 2006, 2012; Marples, 1953; Wiman, 1905a).

Initially, Wiman (1905a, 1905b) described the holotype tarsometatarsi of *Anthropornis* and *Pachypteryx* (junior synonym of the former; Myrcha et al., 2002 and references therein), focusing on the striking size of the material, and the relative size and location of the *foramina vascularia*. This, however, did not include a differential diagnosis of each genus. Later on, some other non-homologous and isolated elements included in the size groups 1 to 4 proposed by Wiman (1905b) were assigned to *Anthropornis nordenksjoeldi* (Marples, 1953), probably based on their size and robustness. Although now obsolete, Wiman's size groups allowed the classification of penguin remains using non-conventional categories (Wiman, 1905b). More recently, an important systematic revision based on the tarsometatarsus provided a revised diagnosis in which *Anthropornis* was unambiguously differentiated from any other penguin (Myrcha et al., 2002).

Currently, and even though there were at least two species recognized in an attempt to analyze its taxonomic diversity (Acosta Hospitaleche et al., 2013; Jadwiszczak, 2006), the number of species of *Anthropornis* is still under debate (Acosta Hospitaleche et al., 2017; Jadwiszczak, 2006). The possibility that a third species has lived sympatrically with *A. grandis* and *A. nordensjkoeldi* in Antarctica during the Eocene is not discarded (see Jadwiszczak, 2006). Only isolated appendicular bones were described for both species of *Anthropornis,* until the finding of a partially complete skeleton assigned to *Palaeeudyptes gunnari* (Acosta Hospitaleche and Reguero, 2010) allowed the reinterpretation of limb elements of *Anthropornis* sp. (Jadwiszczak, 2012). Although Marples (1953) stated that these remains may not belong to the same skeleton, a re-examination of the limbs allowed Jadwiszczak (2012) to confidently assign them to a single individual of *Anthropornis* sp.

The Eocene Marambio/Seymour Island (Fig. 1) penguin record includes isolated cranial elements (Table 1) with a systematic allocation restricted to the family level. On the other hand, the few incomplete skeletons described from the Eocene of Antarctica (Acosta Hospitaleche, 2016; Acosta Hospitaleche and Di Carlo, 2010; Acosta Hospitaleche and Reguero, 2010, 2014; Jadwiszczak, 2012) do not preserve the skull.

Here, new associated remains of a single individual (Fig. 2) with cranium, mandible (Figs. 3, 4), both partial tarsometatarsi (Fig. 5), and some other fragmentary bones are described. The remains were found within Bartonian levels of the Submeseta Formation (Seymour Island), Antarctica (Fig. 1). This partial skeleton has the first cranium reliably assigned to *Anthropornis*, or to any Antarctic penguin species ever. A detailed description of MLP 14-XI-27-84, including osteology, paleoneurology, myological reconstructions, and comments on the inferred paleobiology is provided.

2. Material and methods

2.1. Abbreviations

IAA: Instituto Antártico Argentino, Buenos Aires, Argentina; **MLP**: Museo de La Plata, La Plata, Argentina; **asc**: anterior semicircular canal; **bs**: basis cranii; **cb**: cerebellum; **cc**: capitulum squamosum; **cc**: cotyla caudalis; **cca**: condylus caudalis; **cer**: cerebral hemisphere; **ci**: cisura interhemispherica; **cl**: cotyla lateralis; **cih**: crista intermedia hypotarsi **clh**: crista lateralis hypotarsi; **cm**: cotyla medialis; **cmh**: crista medialis hypotarsi; **cme**: condylus medialis; **cns**: crista nuchalis sagittalis; **cnt**: crista nuchalis transversa; **co**: condylus occipitalis; **col**: cotyla lateralis; **com**: cotyla medialis; **cot**: capitulum oticum; **coq**: corpus ossi quadrati; **cp**: condylus pterigoideus; **e**: externus; **ei**: eminentia intercotylaris; **f**: os frontalis; **fac**: facies articularis cranialis; **fm**: formamen magnum; **fgn**: fossa glandulae nasale; **fl**: facies lateralis; floc: floccu**fm**: facies medialis; **fn**: foramen; **fs**: fossa subcondylaris; **ft**: fossa temporalis; **fvpl**: foramen vasculare proximale laterale; **fvpm**: foramen vasculare proximale mediale; **ie**: inner ear; **ii**: incisura intercapitularis; **l**: lacrimal; **lag**: lagena; **lig**: ligamentum; **lp**: lamina parasphenoidalis; **lpy**: lamina pygostyli **lsc**: lateral semicircular canal; **m**: musculus; **mand**: mandibulae; **med**: medulla oblongata; **ob**: olfactory bulb; **ol**: optic lobe; **pc**: prominentia cerebellaris; **pit**: pituitary; **plp**: processus lateralis parasphenoidalis; **pm**: processus mandibularis; **pmp**: processus medialis parasphenoidalis; **po**: processus oticum; **por**:

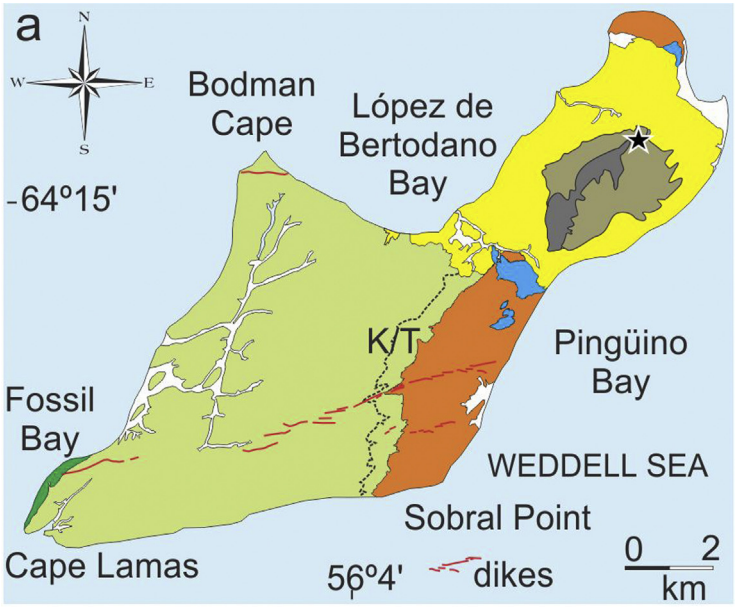
a
N
W
E
S
Bodman Cape
López de Bertodano Bay
-64°15'
K/T
Pingüino Bay
Fossil Bay
WEDDELL SEA
Sobral Point
Cape Lamas
56°4'
dikes
0 2
km

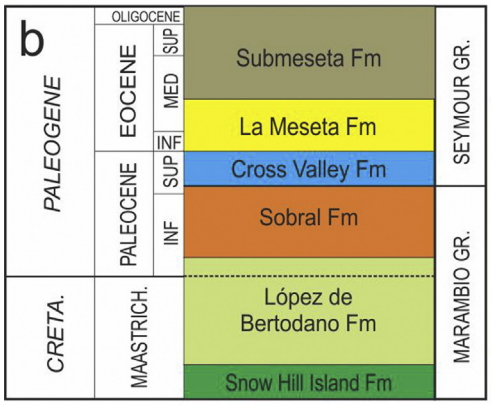
b
PALEOGENE
CRETA.
OLIGOCENE
EOCENE
SUP
MED
INF
PALEOCENE
SUP
INF
MAASTRICH.
Submeseta Fm
La Meseta Fm
Cross Valley Fm
Sobral Fm
López de Bertodano Fm
Snow Hill Island Fm
SEYMOUR GR.
MARAMBIO GR.

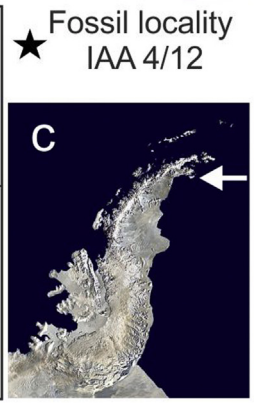
Fossil locality
IAA 4/12
c

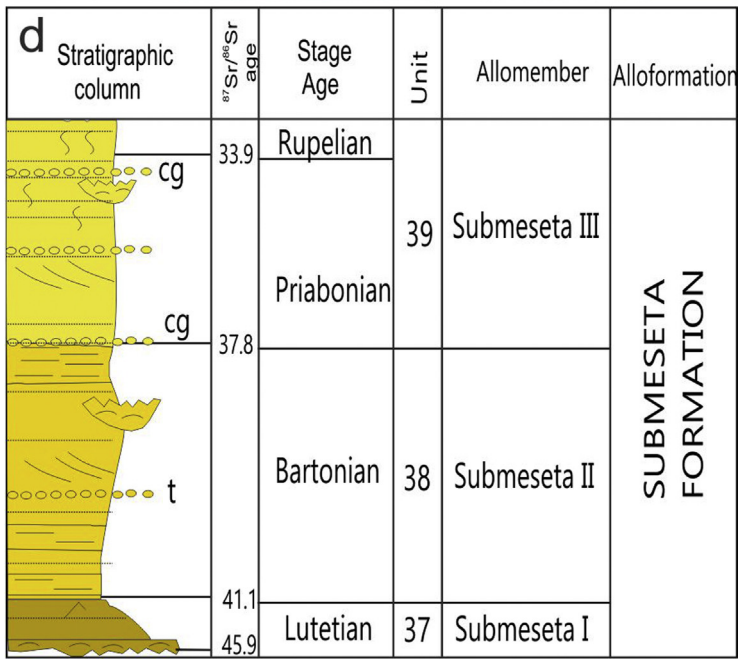
d
Stratigraphic column
87Sr/86Sr age
Stage Age
Unit
Allomember
Alloformation
cg
cg
t
33.9
37.8
41.1
45.9
Rupelian
Priabonian
Bartonian
Lutetian
39
38
37
Submeseta III
Submeseta II
Submeseta I
SUBMESETA FORMATION

Table 1
List of the cranial materials assigned to penguins from Seymour Island, Eocene of Antarctica.
Tableau 1
Liste des matériaux crâniens attribués aux manchots de l'île Seymour, Éocène de l'Antarctique.

Repository number	Material	Reference
IB/P IB-0099	12 cranial fragments	Myrcha et al., 1990
IB/P/B – 0167	Partial cranium	Myrcha et al., 1990
IB/P/B – 0346	Partial cranium	Jadwiszczak, 2006
UCMP 321265	Partial cranium	Ksepka and Bertelli, 2006
UCMP 321208 UCMP 321223 UCMP 318657	Cranial fragments	Ksepka and Bertelli, 2006
MLP 84-II-1-10	Partial cranium	Acosta Hospitaleche and Haidr, 2011
MLP 12-I-20-1	Partial cranium	Acosta Hospitaleche, 2013
MLP 12-I-20-2	Partial cranium	Acosta Hospitaleche, 2013
MLP 12-XII-28-8	Partial cranium	Haidr and Acosta Hospitaleche, 2017b
MLP 14-XI-27-84	Cranium/mandible	Present contribution

processus orbitalis; **pp**: processus postorbitalis; **ppo**: processus paroccipitalis; **proc**: processus; **psc**: posterior semicircular canal; **pu**: processus uncinatum; **pz**: processus zygomaticus; **sc**: sutura costouncinatum; **sm**: symphysis mandibularis; **t**: tuberculum; **tmtc**: tuberositas musculi tibialis cranialis; **tb**: tuberculum basilare; **tp**: tuberculum pseudotemporale; **wu**: wulst.

2.2. Material

MLP 14-XI-27-84 was collected by members of the Museo de La Plata (Universidad Nacional de La Plata) and of the Instituto Antártico Argentino during the summer fieldtrip (2013–2014) to Seymour Island, Antarctica. Bones were mechanically prepared and housed at the División Paleontología Vertebrados of the Museo de La Plata.

2.3. Terminology

Osteological and myological descriptions follow the anatomical terminology proposed by Baumel et al. (1993), complemented by Livezey and Zusi (2006) when necessary. Since MLP 14-XI-27-84 constitutes the first skull assigned to *Anthropornis grandis* with certainty, comparisons with other Paleogene penguins are also given. Measurements were taken with a Vernier caliper of 0.1 mm of increment.

2.4. Anatomical reconstructions

A three-dimensional external scan was performed with a NextEngine 3D Laser Scanner Ultra HD from the División Paleontología Vertebrados (Museo de La Plata). Aretrodeformation of the mesh was performed in Landmark

Fig. 2. Associated material of *Anthropornis grandis* MLP 14-XI-27-84 before its complete extraction from the matrix (scale bar = 10 mm).
Fig. 2. Matériau associé à *Anthropornis grandis* MLP 14-XI-27-84 avant son extraction complète de la matrice (barre d'échelle = 10 mm).

Fig. 1. Location map and stratigraphic column. **a**: Seymour Island, the star points the fossil locality IAA 4/12, where *Anthropornis grandis* MLP 14-XI-27-84 was collected; **b**: lithostratigraphic units showed in the map; **c**: general location of Seymour Island and of the Antarctic Peninsula; **d**: stratigraphic column of the Submeseta Formation; the star indicates the fossil locality IAA 4/12.
Fig. 1. Carte de localisation et colonne stratigraphique. **a** : Seymour Island, l'étoile indique la localité fossilifère IAA 4/12, où *Anthropornis grandis* MLP 14-XI-27-84 a été collecté ; **b** : unités lithostratigraphiques indiquées sur la carte ; **c** : emplacement général de l'île Seymour et de la péninsule Antarctique ; **d** : colonne stratigraphique de la formation Submeseta ; l'étoile indique la localité du fossile IAA 4/12.

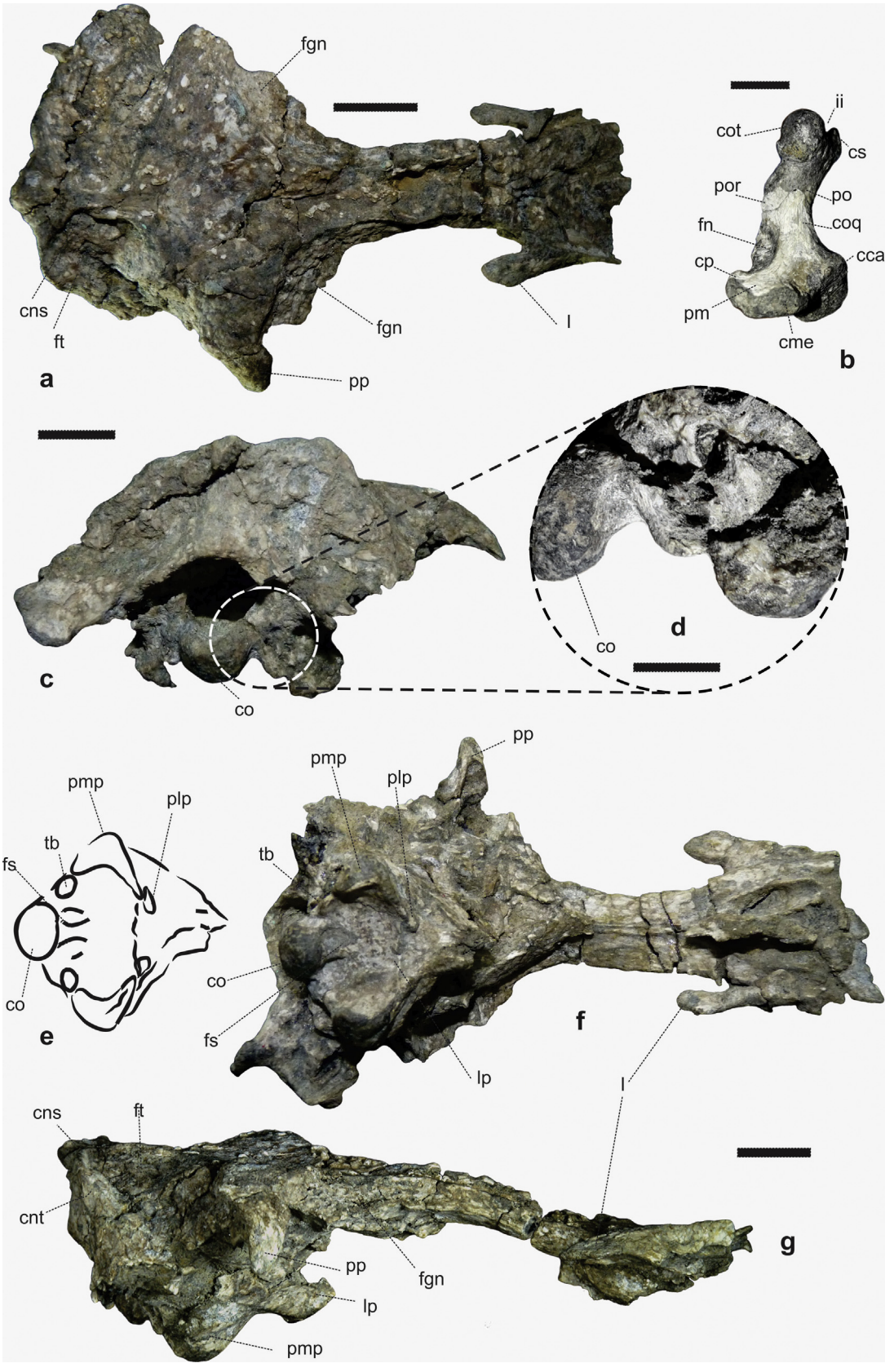
fgn
cns
ft
fgn
l
pp
a
ii
cot
cs
por
po
fn
coq
cp
cca
pm
cme
b
co
c
co
d
pp
pmp
plp
tb
fs
co
e
pmp
plp
tb
co
fs
lp
f
l
cns
ft
cnt
pp
fgn
lp
pmp
g

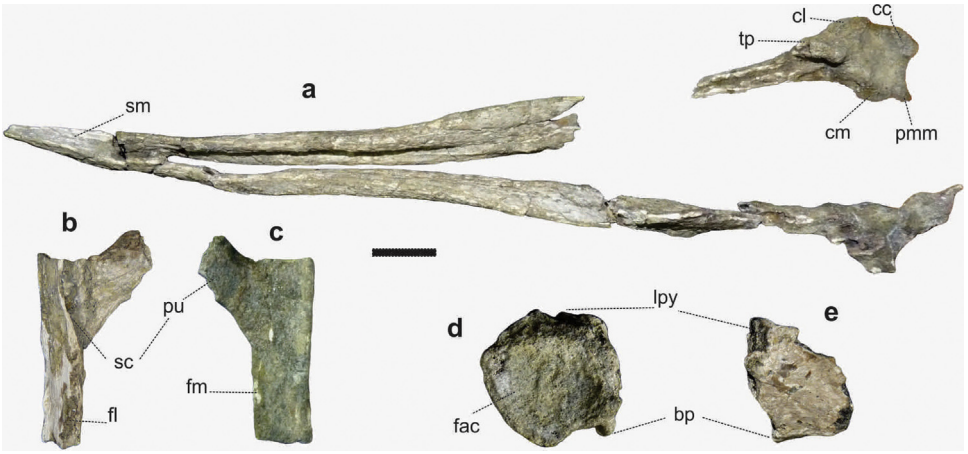

Fig. 4. Mandible, rib and pygostyle of *Anthropornis grandis* MLP 14-XI-27-84. **a**: mandible in dorsal view, deformation of the mandible prevent a strict dorsal perspective; **b**: rib in lateral view; **c**: rib in medial view; **d**: pygostyle in cranial view; **e**: pygostyle in lateral view (scale bar = 20 mm).
Fig. 4. Mandibule, côte et pygostyle d'*Anthropornis grandis* MLP 14-XI-27-84. **a** : mandibule en vue dorsale, la déformation de la mandibule empêche une perspective dorsale stricte ; **b** : côte en vue latérale ; **c** : côte en vue médiale ; **d** : pygostile en vue crânienne ; **e** : pygostile en vue latérale (barre d'échelle = 20 mm).

Editor (Wiley et al., 2007) in order to partially revert the strong taphonomic deformation of the skull (Figs. 6, 7). A microCT scan of the cranium was performed at the Y-TEC facilities (La Plata, Argentina) using a Bruker SkyScan 1173 micro-tomographer, and applying a voltage of 120 kV and a current of 66 μA, resulting in 1117 slices with a thickness of 70 μm. The segmentation of the brain and inner ear was made using the software Materialise Mimics (18.0).

3. Geographic and stratigraphic context

The fossil site IAA 4/12, from where MLP 14-XI-27-84 was collected, is located in the northern sector of Seymour/Marambio Island (Fig. 1a). This island is in the Weddell Sea near the end of the Antarctic Peninsula (Fig. 1c), and remains free of ice during the summer, which makes it one of the best places for paleontological fieldwork in Antarctica. Sediments on Seymour Island are Late Cretaceous to late Eocene/?earliest Oligocene in age, and belong to the lower Marambio Group (composed of the López de Bertodano and Sobral formations) and the overlying Seymour Island Group (Cross Valley, La Meseta, and Submeseta formations) filling the James Ross Basin (Montes et al., 2013).

The specimen MLP 14-XI-27-84 was found within a single block cropping out in surficial deposits of the Submeseta II Allomember of the Submeseta Formation (Montes et al., 2013). These strata are also known as level 38 (Montes et al., 2013), or Telm 7 (Sadler, 1988), and represent the richest unit in terms of fossil penguin diversity and abundance (Fig. 1b, d).

4. Systematic paleontology

Order Sphenisciformes Sharpe, 1891
Anthropornis Wiman, 1905
Anthropornis grandis (Wiman, 1905)
Figs. 3, 4, 5

Material. MLP 14-XI-27-84, partial skeleton including the cranium, mandible, tarsometatarsi, pedal phalanges, several pieces of vertebrae, ribs, and pygostyle.

Locality and horizon. IAA 4/12 locality (Seymour Island), Antarctic Peninsula, West Antarctica (Fig. 1a, c). Priabonian levels of the Submeseta Formation, James Ross Basin (Fig. 1b, d).

4.1. Description and comparisons

Bones are robust and show signs of the osteosclerosis typical of penguins (Houssaye, 2009; Ksepka et al., 2012a; Meister, 1962). The cranium is partially deformed (Figs. 3, 5); it includes the complete calvaria and the *basis cranii externa*, part of the *ossa cranii* and the *cavum tympanicum*, missing the rostrum and palate. The mandible is almost complete.

Both right and left tarsometatarsi are preserved. The left one is complete (Fig. 5), whereas the right one is only represented by a piece of the second and third metatarsal. Other associated elements include fragments of ribs (some of them with fused uncinate processes), cervical and thoracic vertebrae, postzigapophysis of cervical and thoracic vertebrae, pygostyle, six proximal phalanges plus one

Fig. 3. Skull of *Anthropornis grandis* MLP 14-XI-27-84. **a**: cranium in dorsal view (scale bar = 20 mm); **b**: right quadratum (scale bar = 10 mm); **c**: cranium in occipital view (scale bar = 10 mm), the circle indicates the magnified area in d; **d**: close-up of the area indicated in c (scale bar = 5 mm); **e**: schematic drawing of the lamina parashenoidalis and its main processes (same scale as in f); **f**: cranium in ventral view; **g**: cranium in lateral view (scale bar = 20 mm).
Fig. 3. Crâne d'*Anthropornis grandis* MLP 14-XI-27-84. **a** : crâne en vue dorsale (barre d'échelle = 20 mm) ; **b** : quadratique droite (barre d'échelle = 10 mm) ; **c** : crâne en vue occipitale (barre d'échelle = 10 mm) ; le cercle indique la zone agrandie en d ; **d** : gros plan de la zone indiquée en c (barre d'échelle = 5 mm) ; **e** : dessin schématique de la lamina parashenoidalis et de ses processus principaux (même échelle qu'en f) ; **f** : crâne en vue ventrale ; **g**: crâne en vue latérale (barre d'échelle = 20 mm).

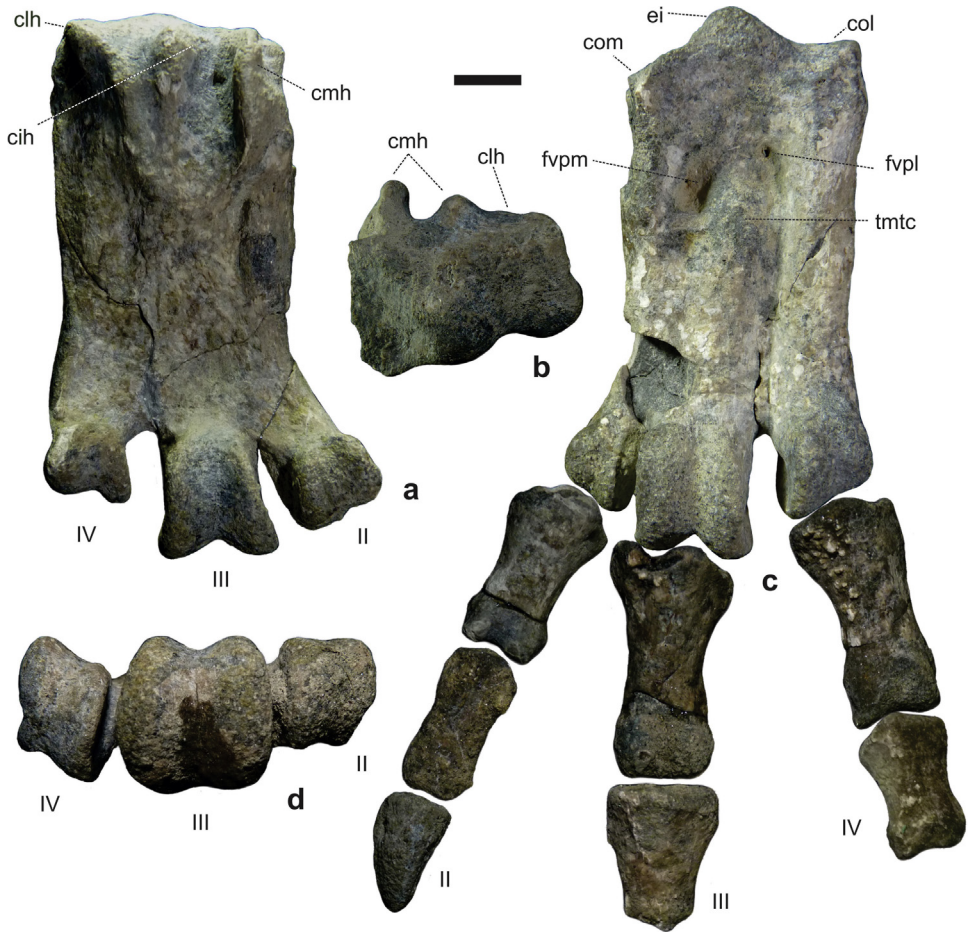

Fig. 5. Left tarsometatarsus of *Anthropornis grandis* MLP 14-XI-27-84. **a**: caudal view; **b**: proximal view; **c**: cranial view; **d**: distal view (scale bar = 10 mm).
Fig. 5. Tarsométatarse gauche d'*Anthropornis grandis* MLP 14-XI-27-84. **a** : vue caudale ; **b** : vue proximale ; **c** : vue crânienne ; **d** : vue distale (barre d'échelle = 10 mm).

phalanx ungualis (Fig. 5c), and several undetermined pieces of bones.

Cranium: *Anthropornis grandis* MLP 14-XI-27-84 is similar in size to MLP 12-I-20-2 (see Table 1 for the complete list of Antarctic crania), but larger than *Muriwaimanu* (Paleocene of New Zealand, Mayr et al., 2017; Slack et al., 2006), *Perudyptes* (Ksepka et al., 2010), *Icadyptes* (Ksepka et al., 2008, although high deformation of the latter makes comparison more difficult), *Inkayacu* (Eocene of Peru, Clarke et al., 2010), or any of the crania found before in Antarctica. The roof of the cranium and the interorbital region are wider and more robust than those in MLP 12-I-20-2, which is the most similar Antarctic cranium (Acosta Hospitaleche, 2013: fig. 5).

The skull roof is a little crushed and the interorbital region is not perfectly aligned with the *crista nuchalis sagittalis* due to dorso-lateral deformation (Fig. 3a, c). The retrodeformed three-dimensional mesh — obtained by the selection of symmetrical points (Fig. 6) — shows an approximation of the skull prior to deformation (Fig. 7). The bridge between both orbitae keeps the same width up to the *os lacrimale*. Neither the suture between the *processus frontalis nasalis* and the *processus frontalis premaxilaris* nor the suture between right and left processes are visible (Fig. 3a).

Both *fossae glandulae nasale* are shallow furrows with a rugose texture that narrow cranially (indeed, the *fossae glandulae nasale* are relatively narrow in all the Antarctic crania). These fossae are medially demarcated by a sharp ridge, which is lower at the caudal end. There is no supraorbital edge at the lateral margin (Fig. 3a). A similar configuration is observed in *Icadyptes, Perudyptes, Inkayacu*, *Muriwaimanu*, and *Sequiwaimanu*.

The orbits are cranio-caudally expanded and limited by a slender and ventro-laterally projected *processus postorbitalis* (which is wider cranio-caudally in *Sequiwaimanu*) and an enlarged *processus supraorbitale lacrimale* (Fig. 3a, c, f). The latter process has a rounded tip that diverges from the sagittal plane toward the caudal end and over the orbit as an expansion of the lacrimal foot (*sensu* Cracraft, 1968). Ventrally, the *processus postorbitalis* is divided by two fossae.

The anterior fossa is postero-medially more expanded and deeper than in MLP 12-I-20-1. Ventrally to this fossa, the scar for the *m. pseudotemporalis superficialis*, in the *area aspera* of the *os laterosphenoidale*, is ventrally more

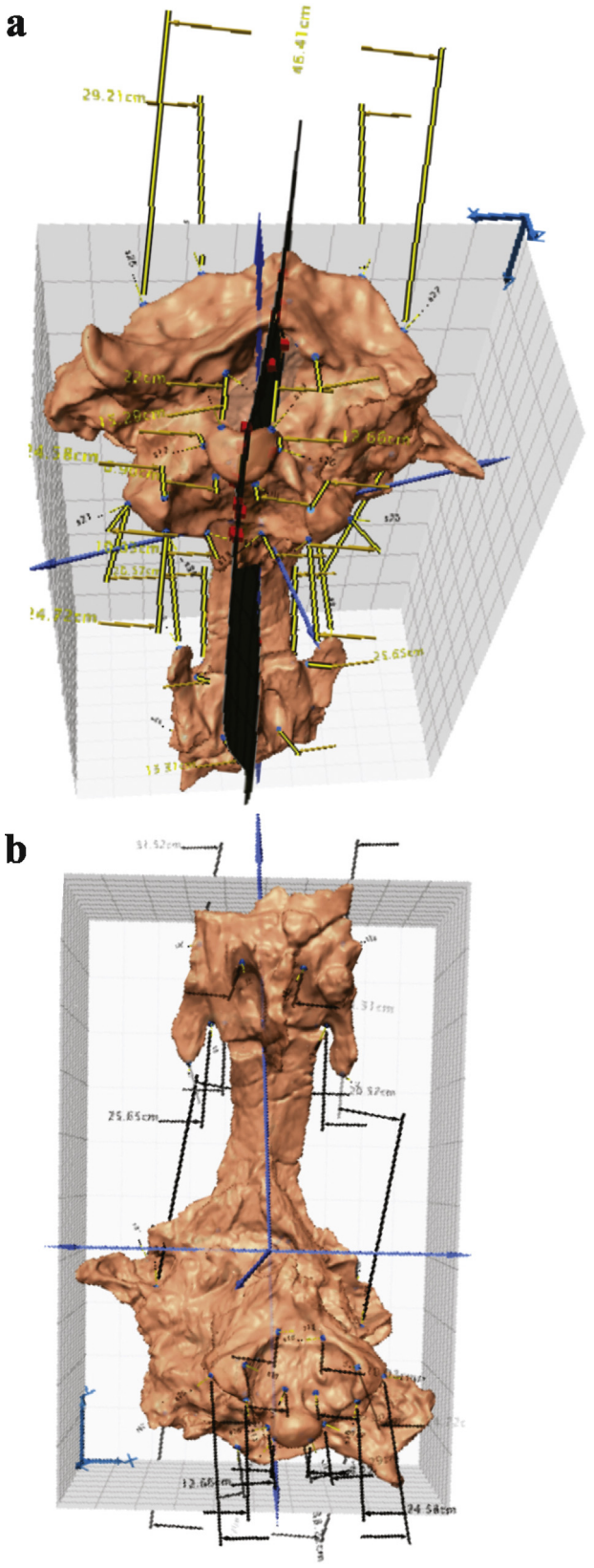
a
46.41cm
29.21cm
25.65cm
b
31cm
25.65cm
12.68cm
24.58cm

extended in *A. grandis* than in other Eocene forms. Beneath this scar, there is another one that includes a fossa deeper than the one of MLP 12-I-20-1. The posterior fossa is also deep, triangular, but rather short in comparison with the former (Fig. 3f). The total area of insertion of the *m. pseudotemporalis superficialis* seems to have been deep, large, and postero-medially more extended than in MLP 12-I-20-1.

The head of the lacrimal is cranio-caudally elongated and, approximately at the middle point of the lacrimal head, the descending process extends ventrally, but also caudally. It ends in an enlarged plate (foot *sensu* Cracraft, 1968) expanded in a *processus supraorbitale lacrimale* (see Cracraft, 1968 for subdivisions of the lacrimal) (Fig. 3a, f). This condition is strongly similar to that observed in Procellariiformes (CAH, pers. obs.).

Although the lacrimal is well developed in all Spheniscidae, the striking enlargement of the *processus supraorbitale lacrimale* appears only in *Anthropornis grandis*, *Icadyptes salasi* (Ksepka et al., 2008: fig. 5A), and *Waimanu tuatahi* (Slack et al., 2006: fig. 1Ab). This projection is not developed in *Kairuku* (Oligocene of New Zealand, Ksepka et al., 2012a), and it cannot be evaluated in *Inkayacu*, or *Sequiwaimanu.* In most penguin species (*e.g.*, *Spheniscus*) the descending process of the lacrimal is notably shorter than in *A. grandis*. Otherwise, the development of the lacrimal plate varies among the species; in *Aptenodytes forsteri* for example, it is larger than in other living genera, but shorter than in *A. grandis*.

The naso-frontal flexure, absent in *Icadyptes* (according to the description of Ksepka et al., 2008) and *Inkayacu*, is present in *A. grandis*. The depression that typically appears in this zone, at least in some extant penguins, is present in *A. grandis*, *Sequiwaimanu,* and seems also present in *Perudyptes*.

The *crista nuchalis sagittalis* is straight and sharp. It separates both *fossae temporale* that extend dorsally reaching the sagittal midline. The whole complexes of *cristae nuchale* draw an inverted U-shaped *fossa temporalis* in dorsal view. At its dorsal end, the *crista nuchalis transversa* constitutes a higher wall compared with the *fossa nuchalis temporalis* (Fig. 3a).

The *fossa temporalis* is slightly crushed, mainly on the left side, but doubtlessly constitutes a wide and deep place for muscular attachment for the *m. adductor mandibulae externus* (Fig. 3a). The *fossa temporalis* is similarly extended in all the materials and is limited by strong borders as in MLP 12-I-20-1, MLP 12-1-20-2, *Icadyptes*, *Perudyptes*, *Inkayacu*, and *Muriwaimanu*. Contrarily, in *Sequiwaimanu* the *fossa temporalis* seems restricted to a more caudal position. In all the other crania compared here, the configuration is similar: the fossae meet each other dorsally at the sagittal line and the strong *cristae nuchale* limits them cranially and caudally. The *os supraoccipitale* extends dorsally, caudal to the *crista nuchalis sagittalis*, constituting an undersized *prominentia cerebellaris*. On the left, a shallow *sulcus vena occipitalis externa* is observed (Fig. 3c).

The foramen rami occipitalis arteria ophtalmica is open at both sides of the prominentia cerebellaris. The condylus occipitalis is kidney shaped and sub-rounded, with a slightly marked incisura medialis condylaris. The processus paroccipitalis is caudally extended, condition that might be caused by dorsal compression (Figs. 3a, 7a). The processus zygomaticus is robust and laterally expanded. The cavum typanicum area is badly preserved, including the cotylae quadratica, which are either not preserved or impossible to visualize (Fig. 3f).

Openings of the *n. hypoglossus* are difficult to determine because this area is badly preserved. However, five openings were attributed to this nerve, besides the larger *foramen nervi vagi* (Fig. 3c, d).

The *lamina parasphenoidalis* is rhomboidal and dorsally located with respect to the *condylus occipitalis*. The *fossa subcondylaris* is deep and divided in left and right sides by a small ridge perpendicular to the *crista basilaris transversa* (Fig. 3e, f). The *lamina parasphenoidalis* is largely expanded and carries strong structures (*processus mediales parasphenoidales*, *p. laterales parasphenoidales*, and *tubercula basilaria*).

The *processus mediales parasphenoidales* are bulky, and cover the lateral boundaries of the *lamina parasphenoidalis*. Each process forms a thick triangle, ventrally rounded and pointing laterally (Fig. 3e, f). These structures are ventrally more prominent than the *condylus occipitalis*, and become slender toward their cranial and caudal ends. Not completely separated from the latter, the *processus laterales parasphenoidales* are more cranio-medially located and remain in contact with the *crista basilaris transversa*. A pair of well-defined *tubercula basilaria* are in the caudalmost end of the *lamina parasphenoidalis*, between the *condylus occipitalis* and the *processus mediales parasphenoidales* (Fig. 3e, f).

Unlike in *Anthropornis grandis*, the *lamina parasphenoidalis* is rectangular in MLP 12-I-20-1, and the whole lateral edges of this lamina are covered by the *processus laterales parasphenoidales*, which are half-moon shaped and reach the *condylus occipitalis* caudally. In *Icadyptes,* the *lamina parasphenoidalis* is sub-circular and the *processus laterales parasphenoidales* are well developed and cranio-caudally expanded, as in *A. grandis*. The *processus mediales parasphenoidales* are missing in *Icadyptes* and MLP 12-I-20-1.

In MLP 12-I-20-1, the *crista basilaris transversa* is more defined than in *A. grandis* and clearly bounders the cranial end of the *lamina parasphenoidalis*. The *fossa subcondylaris* is deeper in *A. grandis* than in MLP 12-I-20-1. The *condylus occipitalis* is blunter and larger in *A. grandis* than in MLP 12-I-20-1.

Fig. 6. Symmetrical points marked on the cranium of *Anthropornis grandis* MLP 14-XI-27-84 to perform the retro-deformation: **a**: caudo-ventral view; **b**: ventral view. The arrows indicate retro-deformation direction; the sagittal plane in black is established from the symmetrical points.
Fig. 6. Points symétriques marqués sur le crâne d'*Anthropornis grandis* MLP 14-XI-27-84 pour effectuer la rétro-déformation. **a** : vue caudo-ventrale ; **b** : vue ventrale. Les flèches indiquent la direction de la rétro-déformation, le plan sagittal en noir s'établissant à partir des points symétriques.

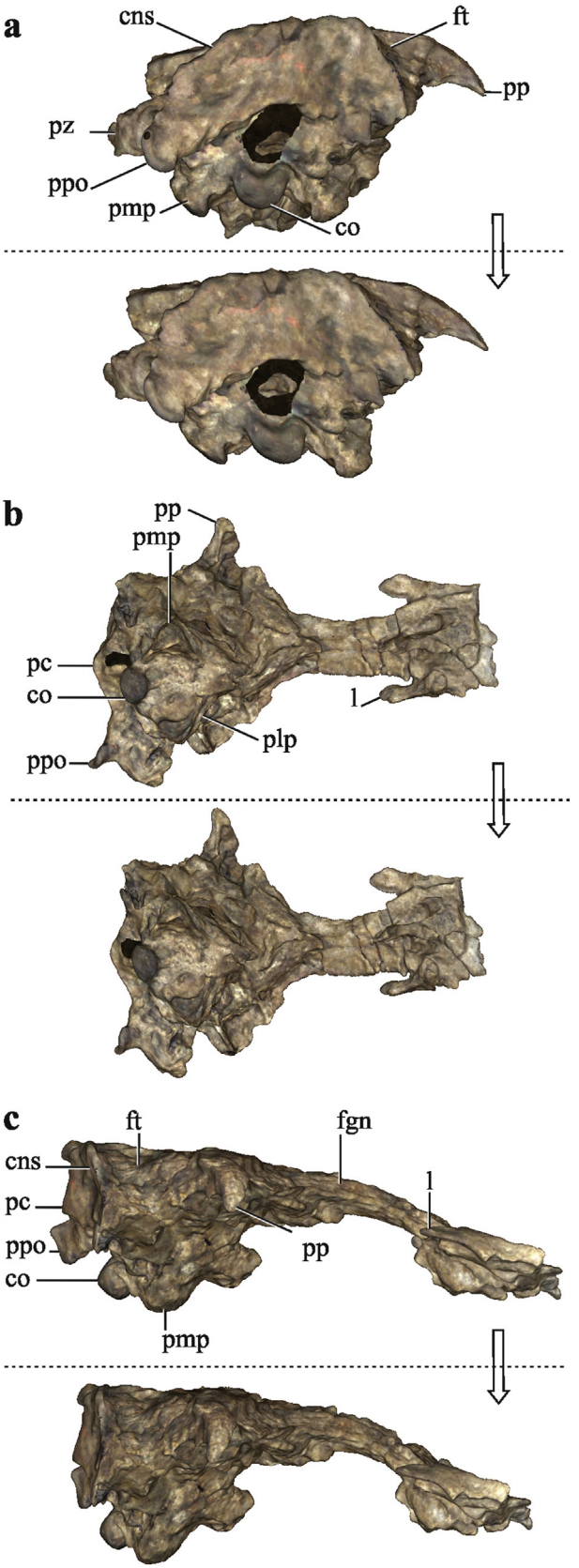
a
cns
ft
pp
pz
ppo
pmp
co
b
pp
pmp
pc
co
l
plp
ppo
c
ft
fgn
cns
pc
l
ppo
pp
co
pmp

The *rostrum parasphenoidalis* is broken, preserving only the caudalmost portion. Parts of the *ossa maxillare* and *premaxillare* are preserved as isolated fragments.

Braincase pneumaticity. A complex series of pneumatic sinuses (*e.g.*, Dufeau, 2011; Elzanowski and Galton, 1991; Witmer, 1997, and references therein) permeate the avian braincase, and a reduction of these sinuses characterizes many diving birds (Ksepka et al., 2012b; Tambussi et al., 2015). Stem fossil penguins have a general pattern for tympanic recess similar to that of extant penguins, except for *Paraptenodytes* (Miocene of Argentina) and MLP 12-I-20-1 (Eocene of Antarctica), which retain the contralateral connection between the paired rostral tympanic recesses called the interaural pathway (Proffitt et al., 2016; Tambussi et al., 2015). This "extra" pneumaticity with respect to extant penguins — the ancestral state in birds except for penguins —, may have had resulted in a potential difference in sound localization in stem taxa (Calford and Piddington, 1988; Proffitt et al., 2016). On the contrary, *Anthropornis grandis* has no relict of the interaural pathway, as shown in Fig. 8a. Also, the conspicuous recess described for MLP 12-I-20-1 as caudal tympanic recess by Tambussi et al. (2015, fig. 7.2) is also present in *A. grandis* (Fig. 8b). The absence of the interaural pathway and the reduction of intracranial pneumaticity in general — regarding other Antarctic fossil penguins — seem to be a derived condition, and *A. grandis* exhibits an intermediate situation.

Quadratum. Left and right quadrates are preserved. The left one preserves the *condylus* of articulation with the mandible and part of the *corpus*, whereas the *processus oticum* and *orbitalis* are missing. The right one is more complete, missing only the *processus orbitalis* (Fig. 3b). Therefore, the *tuberculum subcapitulare*, place of origin of *m. adductor mandibulae externus pars profunda*, is not observed. The quadrates are robust, apneumatic, and massive. They present a sturdy *corpus ossi quadrati* and bulky *condylus caudalis*, *lateralis*, and *medialis*. The *processus oticum* is wide. The *condylus medialis* is ellipsoidal and proportionally larger than in extant forms, and the *processus mandibularis* diverges far from the *corpus ossi quadrati*. The *condylus caudalis* is less extended and closer to the *corpus* than in extant penguins (*e.g.*, *Aptenodytes forsteri*). The *condylus pterygoideus* is well developed and rounded. The right quadratum preserves the tip of the *processus oticum*, where a sub-rounded *capitulum oticum* and the *capitulum squamosum* are separated from each other by a shallow and wide *incisura intercapitularis*. Both *capitula* have a tiny and sharp projection pointing ventrally toward the middle part of the *corpus ossi quadrati*. Two *foramina pneumatica* open at the base of the *processus orbitalis*. The proportional length between the *corpus ossi quadrati* and the *processus orbitalis* cannot be calculated in *A. grandis* because the latter is broken in both sides.

The quadratum of *A. grandis* is dorso-ventrally more extended than that of *Icadyptes* and *Kairuku*. In *Icadyptes*, *condyla* are bulkier and more rounded, and sturdier than in extant penguins, *Kairuku* and *A. grandis*. The *incisura intercapitularis* is similarly developed in *A. grandis* and *Icadyptes*. Although most of the *processus orbitalis* is broken, its base is widened, as in *Kairuku* and differs from the slender *processus* in living forms.

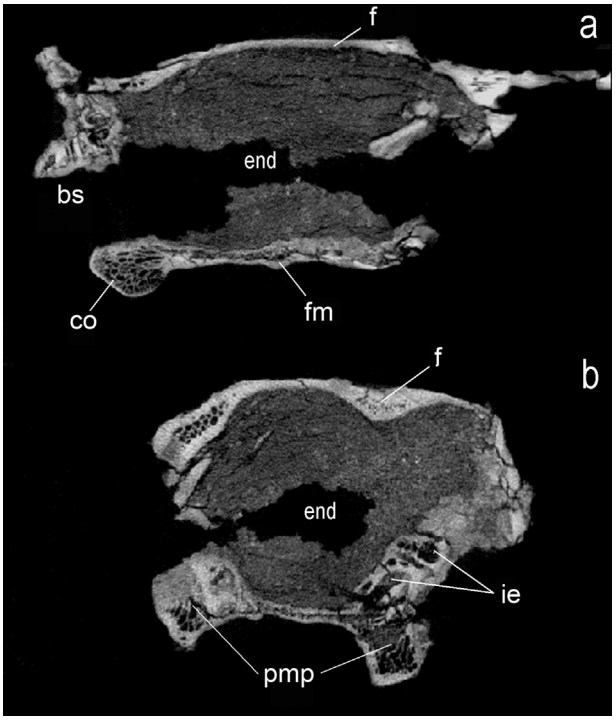

Fig. 8. CT scan slices of the skull of *Anthropornis grandis* MLP 14-XI-27-84 showing the lack of large pneumatic cavities. **a**: sagittal slice; **b**: coronal slice. Not to scale.
Fig. 8. Scanner des coupes du crâne d'*Anthropornis grandis* MLP 14-XI-27-84 montrant l'absence de grandes cavités pneumatiques. **a** : tranche sagittale ; **b** : tranche coronale. Pas à l'échelle.

Mandible. *Rami mandibulae* are slender and extremely elongated (Fig. 4a). The *ramus mandibulae* are incomplete, missing the *processus coronoideus* and the *angulus mandibulae*.

The *pars symphysialis* is similar in extension to that one of *Icadyptes*, *Inkayacu, Muriwaimanu*, and *Sequiwaimanu*; it is convex ventrally and barely concave dorsally. In *Kairuku*, the tip of the mandible is completely different, for it has a moderate ventral deflection, whereas it is straight in all the other compared Paleogene mandibles.

The *cristae tomiale* are sharper at the cranialmost part. In the medial aspect, a deep *sulcus* runs along the *ramus* to its half, where it becomes shallower and disappears leaving a flat surface. The *ramus mandibulae* presents a lingual depression in *Anthropornis grandis*, feature previously described in *Perudyptes* (Ksepka and Clarke, 2010).

Fig. 7. Cranium of *Anthropornis grandis* MLP 14-XI-27-84 showing the original and the retro-deformed images. **a**: occipital view; **b**: ventral view; **c**: lateral view. The arrows indicate the change direction during the retro-deformation process.
Fig. 7. Crâne d'*Anthropornis grandis* MLP 14-XI-27-84 montrant l'original écrasé et les images rétro-déformées. **a** : vue occipitale ; **b** : vue ventrale ; **c** : vue latérale. Les flèches indiquent le changement de direction du crâne déformé lors du processus de rétro-déformation.

However, in the latter, the *ramus* is caudally higher than in *A. grandis*.

Although the articular area is partially covered by sediment, each *cotyla* can be clearly distinguished. The *cotyla medialis* is more ventrally located than the others and it bends medially. The *processus medialis mandibulae* extends medio-caudally as a triangular projection. The *facies articularis parasphenoidalis* is large and similarly expanded to that one in *Inkayacu*. The *cotyla caudalis* is separated from the *cotyla lateralis* by a wide fossa. *Cotylae lateralis* and *caudalis* of the mandible are larger and stronger in *A. grandis* than in *Inkayacu*. Only the *cotyla medialis* presents a similar development in both species.

The *crista transversa fossae* is straight and it limits a wide *sulcus intercotylaris*. The *crista intercotylaris* is rounded and positioned near to the *cotyla medialis*. In *A. grandis*, a strong and rounded process immediately anterior to the *cotyla medialis* is present (Fig. 3g). Due to its position, it might be an exacerbated *tuberculum pseudotemporale* (this tubercle was mistaken in previous contributions for one that lies closer to the ventral margin of the mandible, which might be a *tuberculum* for insertion of the *m. pterygoideus,* see, *e.g.*, Haidr and Acosta Hospitaleche, 2017a), with a degree of robustness not seen in any of the Eocene Antarctic *ramus mandibulae.* In caudal view, the posterior end of the mandible is heart-shaped, with a perfectly rounded *foramen pneumaticum* located in the dorso-medial corner of the *fossa caudalis*. The *foramen pneumaticum* is rounded and larger in *Anthropornis grandis* than in MLP 13-XI-28-199 and in MLP 96-I-6-48.

Costae. Several fragments of ribs are preserved, two of them with a quadrangular *processus uncinatum* fused. Cross-section of the ribs are sub-triangular. The *sutura costouncinatum* appears only on the *facies lateralis* (Fig. 4b, c).

Vertebrae. Several fragments including cervical and thoracic *zygaphophysis caudalis* are present. Unfortunately, the fragmentary state does not allow the comparison of any relevant feature.

Pygostyle. The *basis pygostyli* corresponding to the first fused caudal vertebra is preserved together with the basal part of the *lamina pygostyli* (Fig. 4d, e). The incompleteness of this element does not allow reliable comparisons.

Tarsometatarsus. It is robust and large, with a conspicuous *eminentia intercotylaris* aligned with the third metatarsal, but slightly medially inclined. Accompanying this asymmetry, the *cotyla medialis* is more dorsally placed than the *cotyla lateralis*, which is also smaller (Fig. 5c).

Metatarsals III and IV are parallel along all their extension (Fig. 5a, c), whereas metatarsal II diverges medially (Fig. 5a, c) and *trochlea metatarsi II* is more plantarly located (Fig. 5d). *Trochlea metatarsi II* is the smallest and its trochlear edges are weak. The central *trochlea metatarsi III* is laterally and medially rounded, the most robust, and the most distally projected. Its trochlear edges are the strongest among all the *trochleae*, particularly compared to the medial one. These edges slightly diverge distally and plantarly. *Trochlea metatarsi IV* is the less caudally projected and its trochlear edges are less pronounced than those of *trochlea metatarsi III* (Fig. 5a, c). Due to the lateral leaning of the edges, the medial edge is located at the same level than that of *trochlea metatarsi III*, whereas the lateral edge is lower and plantarly displaced (Fig. 5d).

As typical of the genus, the *foramen vasculare proximale laterale* is considerably smaller and more proximal than its medial counterpart (Fig. 5c). In *Palaeeudyptes*, the other genus of giant penguins from Antarctica, the lateral foramen is large and the medial foramen reduced or absent. Both foramina are separated by a wide third metatarsal III. As described in the revised diagnosis of Myrcha et al. (2002), the proximal end of metatarsal III is clearly lowered in relation to *metatarsalia* II and IV. *Tuberositas musculi tibialis cranialis* is wide, although not well marked.

The *crista medialis hypotarsi* is divided into two short crests, which are more separated from the stronger and wider *crista lateralis hypotarsi*. The last one is aligned with the second metatarsal and extends further distally, broadening at its distal end (Fig. 5a, b).

Measurements. proximal end: dorso-plantar width 28.8 mm; diaphysis: latero-medial width (minimum distance) 33.3 mm; distal end: latero-medial width (trochlear width) 47.1 mm; trochlea metatarsi III: latero-medial width 17.9 mm, dorso-plantar width 22 mm.

Phalanges. The phalanges I, II and the ungual of digiti II, phalanges I and II of digiti III, and phalanges I and II of digiti IV are preserved (Fig. 5c). The first phalanx of digit II is preserved in two pieces. The *facies dorsalis* is barely convex, whereas the *facies plantaris* is concave. The *tuberculum extensorius* is high and leans toward the metatarsal III. The *tuberculum flexorium* extends proximally just a little less than the *t. extensorius*. The *cotyla articularis* is represented by two symmetrical facets separated by a weak vertical rib extended between both *tubercula*. The dorsal extension of the *fovea subtrochlearis* is scarce and continues distally with the *trochlea articularis*. The *caput phalangis* is sub-rounded and the *fovea ligamentaris collateralis* is just marked. The entire *corpus* of the second phalanx of digit II is dorso-plantarly more depressed than the first phalanx. The *phalangis ungualis* surface is completely weathered, and most of its features are erased. Its general morphology represents a cone with an almost flat plantar surface (the *tuberculum flexorium* forms a blunt protuberance that covers the half of this face). The *caput phalangis* has a slight inclination toward the digit III.

The digit III is sturdier than the others, and the first phalanx is particularly massive. The hourglass shape is a little more accentuated, although the proximal end is wider and higher than the distal tip. The *tuberculum flexorium* is very conspicuous, and it indicates the limit between both *cotylae* in the proximal face. The *medial cotyla articularis* is wider than the lateral one. All the other features described before are very similar to this phalanx.

Finally, the first phalanx of digit IV is intermediate in size between the proximal phalanges of digits II and III. The *tuberculum extensorius* leans medially, and the lateral side of the *corpus* is straighter than the medial side. The *cotylae articularis* are deep and symmetrical. The second phalanx follows a similar morphology, although it is dorso-plantarly more depressed.

5. Cranial endocast (Fig. 9)

The cranial endocast of *Anthropornis grandis* is complete, but deformed. The main deformation forces were dorso-latero-ventral, resulting in a somehow more "flatten" cranial endocast. However, some structures, such as the *cisura interhemispherica* (deep straight longitudinal groove separating the cerebral hemispheres medially), both wulsts or sagittal eminences, the cerebellum, partial cerebral hemispheres, the optic lobe, partial pituitary, and right inner ear, can be observed (particularly in dorsal and right lateral views). The volume of the endocranial cast is difficult to determine due to the high degree of deformation. The size of the cerebral hemispheres (48.4 mm in length and 45.5–51.0 mm in width) and wulst (45.5 mm in length and 17.5 mm maximum in width) suggests a volume similar to that of other Antarctic stem penguins, calculated in a range of 27.3–28.8 cm^3 (see Tambussi et al., 2015, tables 1 and 3).

The main axis of the cranial endocast is parallel to the main axis of the skull, as in all crown penguins, fossil stem penguins such as *Paraptenodytes antarcticus*, and *Gavia* (Ksepka et al., 2012b; Paulina-Carabajal et al., 2015; Proffitt et al., 2016; Tambussi et al., 2015). There is a weak lateral expansion of the cerebral hemispheres, a noticeable feature described also for MLP 12-I-20-1 and MLP 12-I-20-2 by Tambussi et al. (2015), which results in a less "heart-shaped" outline in dorsal view (Fig. 9a, b). The length of the cerebral hemispheres is 48.4 mm, whereas the preserved width is 45.5 mm. These measurements are similar to those of MLP 84-II-1-10 (51.5 mm long, 47.5 mm width; Tambussi et al., 2015), being, in turn, larger than the other Antarctic fossil and extant penguins. In *Anthropornis grandis*, the *fissura interhemispherica* is wide and deep, particularly anteriorly, as in other Antarctic penguins (Tambussi et al., 2015), the Miocene *Paraptenodytes* and the Paleocene specimen CM 2013.27.1 described by Proffitt et al. (2016). This trait is not shared with crown penguins.

In *Anthropornis grandis*, there is a well-defined wulst, as in living forms (*e.g.*, *Aptenodytes*, *Spheniscus*), and *Paraptenodytes* and other Eocene Antarctic forms among fossil taxa (Bee de Speroni and Pirlot, 1987; Ksepka et al., 2012b; Tambussi et al., 2015), and opposed to the Paleocene penguin from New Zealand (specimen CM 2013.27.1 described by Proffitt et al., 2016), whose wulsts are markedly smaller. However, as stated for other Eocene Antarctic penguins, this structure is less dorsally expanded than in extant forms. In *A. grandis*, the wulst is elongated, occupying approximately the complete length of the cerebral hemisphere, extending almost to the level of the cerebellum. In extant penguins and *Paraptenodytes*, the wulst is more projected and extends all the way to the level of the *cerebellum* in dorsal view (Tambussi et al., 2015). In *A. grandis*, both wulsts are sub-elliptically shaped in dorsal view, with lateral margins almost parallel (not curved). The clear separation between the wulst and the rest of the cerebral hemisphere indicates that there was a conspicuous *vallecula*. Each wulst is not expanded posteriorly (as is in *Pygoscelis calderensis*, Paulina-Carabajal et al., 2015).

The *cerebellum* is globose, largely exposed in dorsal view and clearly differentiated from the wulsts. The *cerebellum*

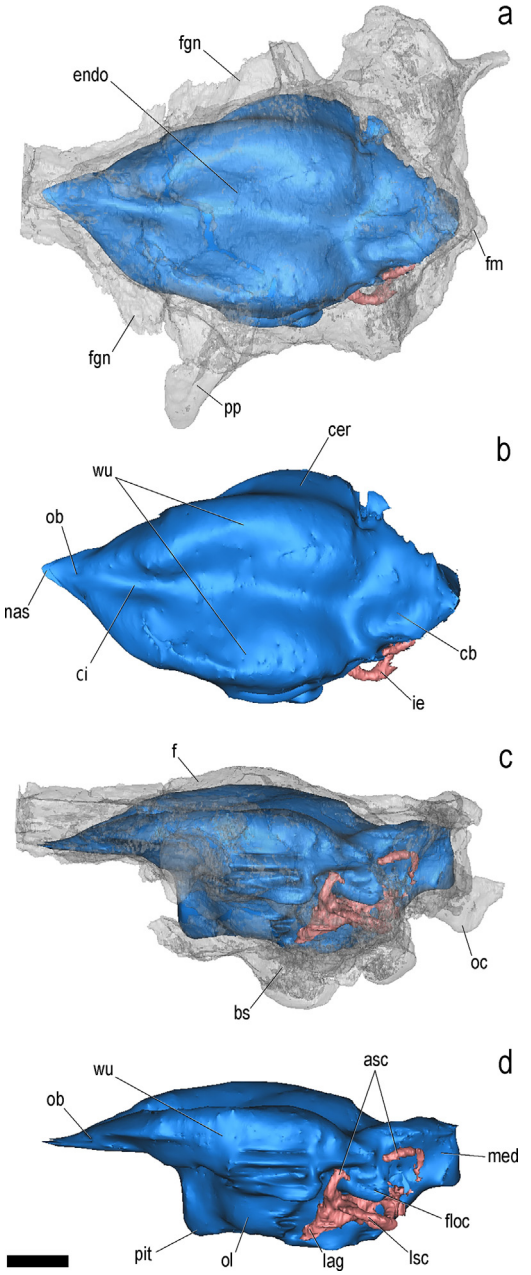

Fig. 9. Digitally rendered skull and cranium endocast of *Anthropornis grandis* MLP 14-XI-27-84. The bone is semi-transparent to allow observation of internal structures. **a, b**: dorsal views; **c, d**: left lateral views (scale bar = 10 mm).
Fig. 9. Endocast crânien et crâne numériquement rendus d'*Anthropornis grandis* MLP 14-XI-27-84. L'os est semi-transparent pour permettre l'observation des structures internes. **a, b** : vues dorsales ; **c, d** : vues latérales gauches (barre d'échelle = 10 mm).

is similar to that described for MLP 12-I-20-1, having a relatively blunt caudal margin and a width greater than that of the *medulla oblongata*. In extant penguins and in *Paraptenodytes*, the *cerebellum* sharply tapers its caudal margin and is narrower than the *medulla oblongata* (Tambussi et al., 2015). The floccular process of the *cerebellum* (*auricula*

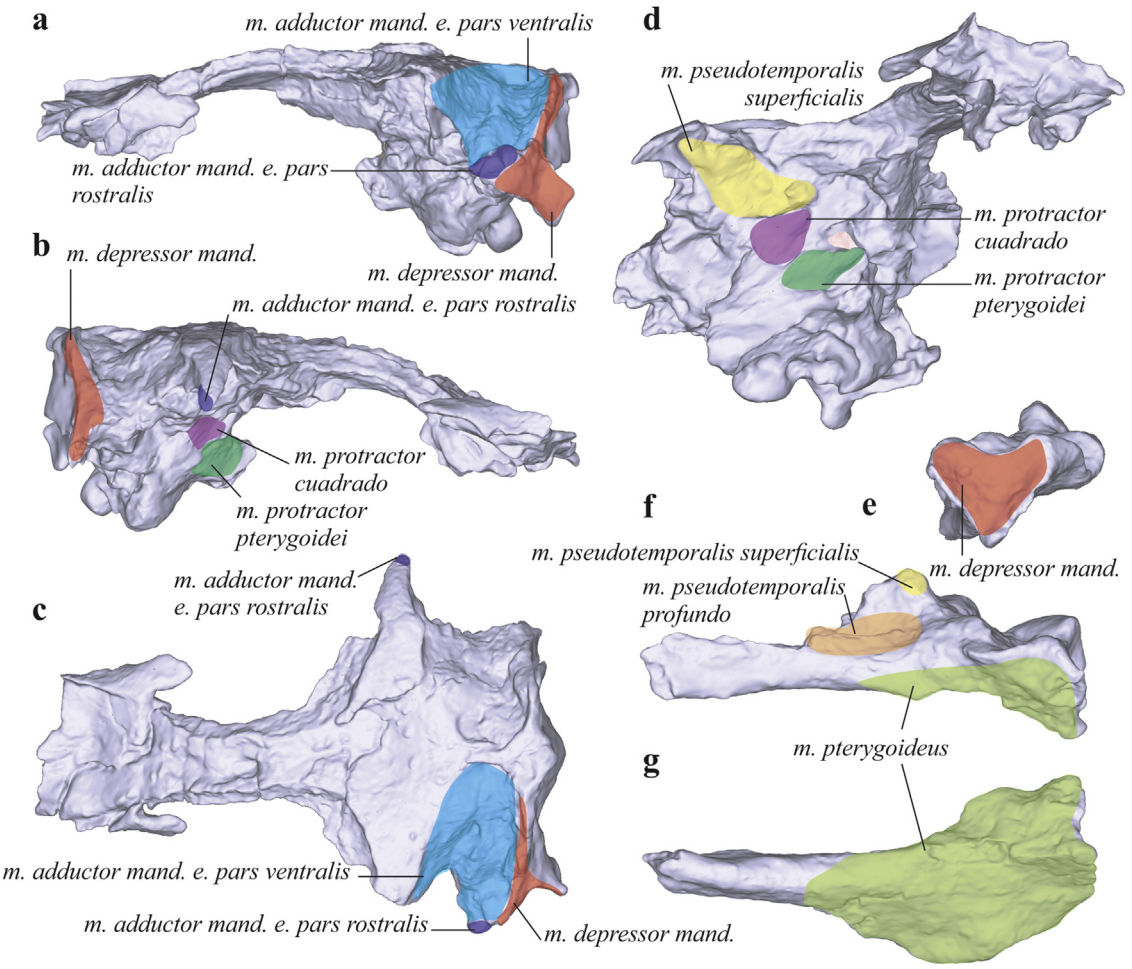

Fig. 10. Muscle attachment areas on the cranium of *Anthropornis grandis* MLP 14-XI-27-84 in **a**: left lateral view; **b**: right lateral view; **c**: dorsal view; **d**: right ventrolateral view; on the right caudal end of mandible in **e**: caudal view; **f**: medial view; **g**: ventral view.
Fig. 10. Zones de fixation musculaire sur le crâne d'*Anthropornis grandis* MLP 14-XI-27-84 en **a** : vue latérale gauche ; **b** : vue latérale droite ; **c** : vue dorsale ; **d** : vue ventrolatérale droite ; à l'extrémité caudale droite de la mandibule: **e** : vue caudale ; **f** : vue médiale ; **g** : vue ventrale.

cerebelli) is a prominent tongue-shaped structure (at least 8.9 mm in length), posterolaterally projected and closely related to the anterior semicircular canal of the inner ear (Fig. 9d). Endocranially, the *auricula cerebelli* is hosted within a large recess, the *fossae auriculae cerebelli*. The size and orientation of the *flocculus* are similar to what has been described for other Eocene Antarctic penguins by Tambussi et al. (2015), particularly MLP 12-I-20-1 and MLP 12-I-20-2, whereas MLP 84-II-1-10 has the longest *flocculus* (12.3 mm long).

The olfactory tracts are markedly short and the olfactory bulbs are relatively small (approximately 7.5 mm in length) and poorly differentiated from the forebrain, as in other penguins (Paulina-Carabajal et al., 2015; Tambussi et al., 2015) (Fig. 9b). The olfactory ratio (OR) calculated for *Anthropornis grandis* is about 15.5%, similar to that calculated for *Spheniscus magellanicus* (16.4%) by Tambussi et al. (2015), and smaller than that calculated for the extinct MLP 12-I-20-1 (35%) and *Paraptenodytes* (24.5%).

The optic lobe is clearly visible in the right side of the cranial endocast. They are relatively well developed as in other living and extinct birds (Paulina-Carabajal et al., 2015; Walsh and Milner, 2011a, 2011b) and posteroventrally located regarding the cerebral hemispheres. Ksepka et al. (2012b) stated that the amount of variation in the form of the optic lobe within Spheniscidae is small compared with that between penguins and other groups.

The posterior region of the pituitary is preserved as a rounded structure at the base of the endocasts. As in the other Eocene (Tambussi et al., 2015) and Paleocene (Proffitt et al., 2016) penguins, the pituitary seems larger than in extant penguins. There are no observed neurovascular canals in the endocasts.

The inner ear is dorso-ventrally deformed, but several segments of the three semicircular canals, and the lagena, are preserved (Fig. 9a–d). It seems to exhibit the general avian morphology with large and slender semicircular canals and a long and slender lagena. It is likely that the orientation of the semicircular canals, particularly the anterior semicircular canal, is oblique relative to the anteroposterior axis of the skull, as in *Pygoscelis*. The semicircular canals are robust and the diameter of the tubes measures

approximately 2.2 mm, similar to the robust semicircular canals of the Eocene Antarctic stem penguin MLP 12-I-20-1 (Tambussi et al., 2015), but larger than that in MLP 84-II-1-10. The anterior semicircular canal is the largest (Fig. 9d); it is oval and posteriorly inclined. It is not taller than the posterior semicircular canal. The angle between the asc and psc (in dorsal view) is slightly larger than 90 degrees, although, because of the deformation, this measurement cannot be confirmed. The lateral semicircular canal is complete and corresponds to an almost circular shape. As stated by Tambussi et al. (2015), the Antarctic fossil penguins have stouter (wider in diameter relative to overall labyrinth size) semicircular canals than in *Paraptenodytes* and the sampled extant penguins so far.

6. Muscular reconstruction

The temporal region, the *area aspera* on the orbital region, as well as the *processus coronoideus*, and a *processus* anterior to the articulation in the *ramus mandibulae* are conserved. They are all indicative of the development of some of the cranial muscles.

The *m. adductor mandibulae pars rostralis* would have had its surface of origin in a very robust and laterally extended *proc. postorbitalis*. Caudally, the stout *proc. zygomaticus*, which has a similar shape in extant forms, would have been its other point of origin. The plausible insertion of *m. adductor mandibulae pars rostralis* on the *proc. coronoideus* is not preserved.

The *m. adductor mandibulae pars ventralis* (Fig. 10a, b, c) origins on the *fossa temporalis* in extant forms. In *A. grandis,* this fossa is wide, deep, and reaches the sagittal plane forming a *crista sagittalis* (Fig. 3a). *Spheniscus* is the only extant penguin that develops a sagittal crest that is, however, significantly shorter than that of the Eocene forms. The fossa is larger and deeper than in living penguins, except again maybe in *Spheniscus.* The *proc. orbitalis*, which is the lateral limit of its development in extant forms is, as described above, more laterally extended than in any extant species. All of these features would be indicative of a robust and well-developed muscle with a much larger cross-sectional area than in any living species.

The *m. depressor mandibulae* attaches on the *crista nuchalis transversa* (Fig. 10a, b, c) in extant forms. This crista is thicker in *Anthropornis* than in modern species, and would have constituted a strong line of attachment for this muscle. The *m. depressor mandibulae* inserts on the *processus retroarticularis* (Fig. 10c), which in *Anthropornis grandis* is triangular, short, and wide, constituting a large area of origin. However, in comparison with extant forms, this area of insertion is smaller in *A. grandis*. Its lever arm would have been also shorter compared with extant forms such as *Spheniscus,* whose *processus retroarticularis* extends farther posteriorly. The *m. pseudotemporalis superficialis*, whose place of origin is on the *area muscularis aspera* on the *os laterosphenoidale* in living penguins, is preserved on the specimen (Fig. 10d). Its origin would have extended onto a *fossa* that lies underneath the *proc. postorbitalis,* condition not present in extant forms. The putative *tuberculum pseudotemporalis*, insertion point of *m. pseudotemporalis superficialis* (Fig. 10f) might indicate the presence of a strong tendon making contact, strengthening the fleshy insertion of the muscle in the *ramus mandibulae*. In extant forms, this *tuberculum* is more delicate and sometimes hard to identify. Regarding the *m. protractor quadrati*, its origin in the *area muscularis aspera* of the *os laterosphenoidale,* immediately ventral to that of the *m. pseudotemporalis superficialis* (Fig. 10b, d), presents a deep fossa that is clearly visible in the right side. This area of origin suggests that this muscle would have also been well developed.

Both palatines and pterygoids are missing, which is in detriment of a consistent reconstruction of the *m. pterygoideus*. The *tuberculum* in which the tendon of the *m. pterygoideus* Part M (*sensu* Zusi, 1975) inserts (Fig. 10f, g) is much more robust than in extant forms, but less extended than in other Eocene mandibles such as MLP 92-II-2-115a, MLP 96-I-6-48, 13-XI-28-199, and 94-III-15-16a; these observations might be biased by the preservation state of the artefacts. The *processus medialis* of the mandible is well developed (area of attachment of the other parts of this muscle). It is very different to that of living forms, lacking the characteristic hook and extending caudally as opposed to the lateral development in extant forms. Because of these differences, the degree of development of this muscle cannot be certainly affirmed. The *m. adductor mandibulae externus pars profunda*, *m. pseudotemporalis profundus*, and the *m. protractor pterygoidei* could not be reconstructed, because both origin and insertion area lacking, or were unidentified.

7. Discussion and conclusions

MLP 14-XI-27-84 is the first Antarctic skull associated with postcranial elements and, therefore, the first opportunity to make an accurate systematic assignment based on the tarsometatarsus. This specimen, the largest penguin cranium discovered so far, is classified as *Anthropornis grandis*, a giant species that lived in Antarctica during the Eocene. However, according to our knowledge of the giant forms, larger skulls are yet to be discovered.

The beak of this specimen (according to the mandible length) is elongated and slender as in other stem penguins, and the neurocranium is proportionally smaller than that of the extant species. Dimensions of the *condylus occipitalis* and the *foramen magnum*, however, are congruent with a large cranium and neck. Indeed, these proportions are widely extended among large and giant penguins during the Paleogene.

7.1. Secondary support of the mandible

The contact between the *processus medialis parasphenoidalis* (in the *lamina parasphenoidalis*) and the *facies articularis parasphenoidalis* (in the *processus medialis mandibulae*) works as a supplementary bony support of the mandible (Bock, 1960). This articulation is medial to the quadrate-articular joint and exists in many diverse groups of birds (*e.g.*, *Macronectes*), according to our own observations. On the contrary, this abutment is absent in many other birds (*e.g.*, *Oceanites*). In *Anthropornis grandis*, this structure is unusually robust. It was assumed that this

medial brace of the mandible serves to prevent the disarticulation of the mandible from the cranium (Bock, 1960). For that reason, it would be only necessary in birds that catch their prey or break the food by rapid movements of the head. If disrupting forces are strong enough, the medial brace of the mandible could compensate a deficient primary articulation with the *condyla* of the quadrate. It could be summarized that the functionality of this medial brace is determined by the kind of movements to which the joint is subject, the magnitude of the disruptive forces (during feeding), and the efficiency of the quadrate-articular joint (given by the morphology of the quadrate *condyla* and the mandibular *cotylae*).

MLP 14-XI-27-84 is similar to morpho-type 2 of Haidr and Acosta Hospitaleche (2012) because the *cotyla lateralis* is clearly separated from the *cotyla caudalis*. This morphology gives a greater stability and firmness to the mandibular articulation during sudden movements. Contrarily, in the morpho-type 1, the *cotyla lateralis* is merged with the *cotyla caudalis*. This condition was described for crustacivores (Haidr and Acosta Hospitaleche, 2012).

Although the quadrate in *A. grandis* is robust and each *condylus* is perfectly defined and separated from each other, they might be not rounded and bulky enough to resist the destabilizing forces. The great development of the *processus medialis parasphenoidalis* and of the *facies articularis mandibulae* could properly function as a reinforcing to prevent disarticulation during the capture and handling of prey.

In all birds, two muscles attach on the *processus medialis mandibulae*: the *m. depressor mandibulae* inserts along the posterior edge, and the *m. pterygoideus* attaches on its anterior surface. Consequently, the enlargement of this surface would benefit the strength of any of these muscles. As it was pointed before, the additional bony support given by this process would be a preadaptation of the mentioned process (Bock, 1959, 1960).

7.2. The significance of the fossa glandulae nasalis morphology

All the known fossil and living penguins develop a *fossa glandulae nasale* for the location of the salt gland. However, the shape and the development degree of the *fossa glandula nasale* are not clear indicators of the salt gland size (Ibañez, 2009). The supraorbital margin boundering laterally the *fossa glandulae nasale* is present in *Pygoscelis*, *Eudyptes*, and *Megadyptes,* penguins with a broad diet range. On the contrary, the piscivorous *Spheniscus, Eudyptula,* and *Aptenodytes* have the *sulcus* laterally opened, and the salt gland partially resting on the orbit (Ibañez, 2009). A similar condition appears in all the Paleogene taxa (including *Anthropornis* MLP 14-XI-27-84).

7.3. Muscular reconstruction: the cranio-cervical muscles

All the Eocene Antarctic crania (MLP 12-XI-1-1, MLP 12-XI-20-1, MLP 84-II-1-10, and UCMP 321265) present a wide *fossa temporalis* with a deep posterior portion, indicative of a large *m. adductor mandibulae externus*; the situation of *Anthropornis grandis* is not different. This large and deep area of insertion is comparable with that of other Eocene forms such as *Perudyptes devriesi*, *Icadyptes salasi* (Clarke et al., 2007), and also to *Waimanu tuatahi* (Proffit et al., 2016), as well as of geologically younger penguins such as *Paraptenodytes antarcticus* (Ksepka et al., 2012b), and *Spheniscus* (Stucchi et al., 2003).

Another muscle involved in the closing of the jaws is the *m. pseudotemporalis superficialis* (Fig. 10b), which place of both origin and insertion are more robust and well developed than in any of the other Antarctic Eocene forms (of the preserved material) or any extant forms. The biting force would have been powerful, with strong muscles that had large cross-sectional muscle areas. The situation of the *m. depressor mandibulae* (Fig. 10a) would have been different, having similar size with extant forms and a lever arm that would have been relatively short, a condition similar to *Pygoscelis*.

The origin point of the *m. protractor quadrati* indicates a conspicuous muscle that was contained in a much deeper fossa than that found in MLP 12-I-20-1 or extant species. This muscle moves the quadrate, lifting the upper beak (Zusi, 1975).

The presence and the development degree of the *tubercula basilaria* in *Anthropornis grandis* draw attention, especially because they are absent or inconspicuous in extant penguins (they may coincide with the *processus mediales parasphenoidales* according to Baumel et al., 1993). After examination of several specimens of modern penguins, we can establish that these structures are slightly developed (*e.g.*, *Aptenodytes forsteri*) or simply lacking (*e.g.*, *Spheniscus magellanicus*). The presence and development of these tubercles might be correlated with a functional demand of the neck muscles to efficiently support the skull. The *tubercula basilaria* appear in taxa not phylogenetically related, such as *Stercorarius maccormicki* (Charadriiformes), *Pygoscelis adeliae* (Sphenisciformes), and *Cathartes aura* (Cathartiformes), among others. These structures are the attachment area of cranio-cervical *m. rectus capitis dorsalis* and are typically more developed in long-skulled birds (Baumel et al., 1993), like the noticeably elongated skull of the specimen *Anthropornis grandis* here described. But, what does it means in functional terms? The *M. rectus capitis dorsalis* is, in fact, a series of discrete slips (converging towards the insertion) that originate from the anterolateral surface of the cervical vertebra C1, and transverse processes of cervical vertebrae C1–C6. This muscle inserts on the *tubercula basilaria*, if developed, or just in a rugose scar of the *lamina parasphenoidalis*. The *m. rectus capitis dorsalis* is responsible for head ventro-flexion relative to the neck (Snively and Russell, 2007a).

As it was suggested for dinosaurs (Snively and Russell, 2007b), a large insertion area (represented here by *tubercula basilaria*) may indicate a large cross-sectional area for *m. rectus capitis dorsalis* and a relatively more forceful contraction for the ventral and ventrolateral flexion of the head. This is consistent with the morpho-functional requirements that a predator like *Anthropornis grandis* would have had during capturing and handling its prey.

The interdependence of numerous adaptations of the head and neck was already noticed by Zusi (1962), who

proposed the treatment of their totality as an adaptive complex for feeding. A set of characters observed in many penguins can be understood as adaptations for feeding specializations, *e.g.*, innervation of mandible (for detecting prey), hypertrophy of jaw, curvature of the rostrum, and increment of kineticism (for striking prey), and a well-developed *m. adductor mandibulae* (for holding prey). However, some other features observed in *Anthropornis grandis*, such as the broad shape of the quadrate condyles and the increased contact of the mandibular processes and the *lamina parasphenoidalis*, are clearly developed for stabilization of jaws and head.

The development of a wide and deep *fossa temporalis*, a small neurocranium, a robust and large *condylus occipitalis*, and a long and spear-like beak, are among the most conspicuous features. It has been proposed that the Paleogene penguins would have caught large prey by spearing (Ksepka and Bertelli, 2006; Olson, 1985), similar to the strategy of *Podiceps* (Chávez Hoffmeister, 2018). In this regard, whilst extant penguins depend on a powerful biting force, it was suggested that it would not be as important in Paleocene species (Chávez Hoffmeister, 2018). However, *Anthropornis* possess a wide and deep area of origin for the *m. adductor mandibulae externus*, which is the main muscle involved in the biting force. A similar condition appears in *Podiceps major, Aechmophorus*, and other podicipediforms. This is consistent with the development of voluminous and strong muscles. Whether by harpooning or biting, Paleocene penguins would still be in the need of strong forces for catching their prey.

7.4. Paleoneurology

The novel information on the cranial endocast of *Anthropornis grandis* reveals the relative proportions and orientation of the telencephalon, which resemble those of other Miocene Antarctic stem penguins (Tambussi et al., 2015) and the Paleocene penguin from New Zealand (Proffitt et al., 2016). This includes the poor lateral expansion of the cerebral hemisphere, the relative large development of the wulst, and the overlap between the cerebral hemispheres and the *cerebellum* in lateral view (Proffitt et al., 2016 and references therein).

As in the other studied Antarctic fossil penguins and the Paleocene penguin from New Zealand (Proffitt et al., 2016), the development of many structures of the cranial endocasts, such as the wulst and the *flocculus* of the *cerebellum*, is similar in extant penguins and in volant birds (Ksepka et al., 2012b); this is, in turn, consistent with the need for penguins to maneuver in complex three-dimensional space (Tambussi et al., 2015). Prominent *flocculi* seem to be a general feature for diving taxa. Given that most Eocene penguins were piscivorous (Acosta Hospitaleche, 2013), differences are not evidenced in the size of the *flocculus* of the *cerebellum*, nor in the inner ear, when compared to *Pygoscelis* (crustacivores forms) *Spheniscus* or *Aptenodytes* (piscivorous forms) — and therefore this structure is not helpful to better understand the paleobiology of *Anthropornis*. Also, the lack of cerebellar fold impressions on the endocasts is a trait shared by all wing-propelled diving birds (see Tambussi et al., 2015, and discussion therein).

In the case of *Anthorpornis*, the relative large size of the semicircular canals could be associated with diving skills, whereas the relatively more robust canals may indicate a slight difference in maneuverability when compared to extant penguins. The lagena is elongate and conical, not distally expanded, as described for other extinct and extant penguins (e.g., Paulina-Carabajal et al., 2015; Tambussi et al., 2015). Regarding the olfaction, Tambussi et al. (2015) calculated the olfactory ratios for MLP 12-I-20-1, which had the greatest olfactory ratio for any sampled penguin, suggesting that higher levels of olfactory sensitivity may have characterized basal penguins compared with extant taxa. Although the relative importance of olfaction has not been quantified in penguins yet, the higher olfactory ratio in MLP 12-I-20-1 has been interpreted by the mentioned authors as a primitive trait. The olfactory bulbs are not clearly visible in the CT scans of *A. grandis*; yet, the estimated size and shape (see Fig. 9) suggest an olfactory ratio markedly similar to that of MLP 12-I-20-1.

Although the transitions of the neuroanatomy associated with the evolution of flight have been subject to extensive research, the shift to a diving ecology is less understood, and the correlation between diving and brain morphology remains poorly understood (Tambussi et al., 2015 and references therein). While there are many similarities in braincase and endocranial anatomy between *Anthropornis grandis*, MLP 12-I-20-1, and MLP 84-II-1-10, the former exhibits a lesser degree of cranial pneumaticity and lacks the interaural connection. It is unclear for us if this difference responds to inter- or intraspecific variability.

Acknowledgments

Antarctic field trip was completely funded by Dirección Nacional del Antártico and the Instituto Antártico Argentino, and logistic support in the field was provided by Fuerza Aérea Argentina. Partial help was provided by the Consejo Nacional de Investigaciones Científicas y Tecnológicas and Universidad Nacional de La Plata (N838). Leonel Acosta (Museo de La Plata) prepared the fossil, María Bernarda Epele and Mariano Cipollone (Y-TEC) made Micro-CT scans, and Agustín Ruella together with Nicolás Bauzá (Museo de La Plata) performed the retro-deformation analyses. CAH is particularly grateful to Oceanwide Expeditions, Vlissingen (NL) for financial support. This project was partially funded by PICT-E 0080 (to División Paleontología Vertebrados, MLP), UNLP N838 (to CAH), and PICT-2016-0481 (to APC). María Florencia Sosa improved the English grammar. Three anonymous reviewers made important comments that improved our manuscript.

References

Acosta Hospitaleche, C., 2013. New crania from Seymour Island (Antarctica) shed light on anatomy of Eocene penguins. Pol. Polar Res. 34, 397–412.

Acosta Hospitaleche, C., 2014. New penguin giant bones from Antarctica: systematic and paleobiological significance. C. R. Palevol 13, 555–560.

Acosta Hospitaleche, C., 2016. Paleobiological remarks on a new partial skeleton of the Eocene Antarctic penguin *Palaeeudyptes klekowskii*. Ameghiniana 53, 269–281.
Acosta Hospitaleche, C., Di Carlo, U., 2010. The coracoids in functional and morphological studies of penguins (Aves, Spheniscidae) of the Eocene of Antarctica. Riv. Ital. Paleontol. S 116, 23–34.
Acosta Hospitaleche, C., Haidr, N., 2011. Penguin cranial remains from the Eocene La Meseta Formation, Isla Marambio (Seymour Island), Antarctic Peninsula. Antarct Sci. 23, 369–378.
Acosta Hospitaleche, C., Reguero, M., 2010. First articulated skeleton of *Palaeeudyptes gunnari* from the late Eocene of Isla Marambio (Seymour Island), Antarctica. Antarct. Sci. 22, 289–298.
Acosta Hospitaleche, C., Reguero, M., 2014. *Palaeeudyptes klekowskii*, the best preserved penguin skeleton from the Eocene–Oligocene of Antarctica: Taxonomic and evolutionary remarks. Geobios 47, 77–85.
Acosta Hospitaleche, C., Reguero, M., Scarano, A., 2013. Main pathways in the evolution of the Paleogene Antarctic Sphenisciformes. *J. S. Am. Earth Sci.* 43, 101–111.
Acosta Hospitaleche, C., Reguero, M., Santillana, S., 2017. *Aprosdokitos mikrotero* gen. et sp. nov., the tiniest Sphenisciformes that lived in Antarctica during the Paleogene. Neues Jahrb. Geol. Palaontol. Abh. 283, 25–34.
Baumel, J.J., King, A.S., Breazile, J.E., Evans, H.E., Vanden Berge, J.C., 1993. Handbook of avian anatomy: Nomina Anatomica Avium, Publication No. 23. Publications of the Nuttal Ornithological Club, Cambridge, Massachusetts.
Bee de Speroni, N., Pirlot, P., 1987. Relative size of avian brain components of the Magellanic Penguin, the Greater Rhea, and the Tataupa Tinamou. Mar. Ornithol. 15, 7–22.
Bock, W.J., 1959. Preadaptation and multiple evolutionary pathways. Evolution 13, 194–211.
Bock, W.J., 1960. Secondary articulation of the avian mandible. Auk 77, 19–55.
Calford, M.B., Piddington, R.W., 1988. Avian interaural canal enhances interaural delay. J Comp. Physiol. 162, 503–510.
Chávez Hoffmeister, M., 2018. Ocupación del morfoespacio y estrategias alimenticias en pingüinos y otras aves acuáticas , Actas VI Congreso Latinoamericano de Paleontología de Vertebrados, Villa de Leyva, p. 71.
Clarke, J.A., Ksepka, D.T., Stucchi, M., Urbina, M., Giannini, N., Bertelli, S., Boyd, C.A., 2007. Paleogene equatorial penguins challenge the proposed relationship between biogeography, diversity, and Cenozoic climate change. Proc. Natl. Acad. Sci. USA 104, 11545–11550.
Clarke, J.A., Ksepka, D.T., Salas-Gismondi, R., Altamirano, A.J., Shawkey, M.D., D'Alba, L., Baby, P., 2010. Fossil evidence for evolution of the shape and color of penguin feathers. Science 330, 954–957.
Cracraft, J., 1968. The lacrimal-ectethmoid bone complex in birds: a single character analysis. Amer. Midl. Naturalist. 80 (2), 316–359.
Dufeau, D.L., 2011. The evolution of cranial pneumaticity in Archosauria: patterns of paratympanic sinus development (Ph.D. dissertation). Ohio University.
Elzanowski, A., Galton, P.M., 1991. Braincase of *Enaliornis*, an Early Cretaceous bird from England. J. Vert. Paleontol. 11, 90–107.
Haidr, N., Acosta Hospitaleche, C., 2012. Feeding habits of Antarctic Eocene penguins from a morphofunctional perspective. Neues Jahrb. Geol. Palaeontol. Abh. 263, 125–131.
Haidr, N., Acosta Hospitaleche, C., 2017a. Fossil penguins beaks from the Eocene of Antarctica: new materials from La Meseta Formation. Vol. Especial Rev. MACN 7, 57–68.
Haidr, N., Acosta Hospitaleche, C., 2017b. A new penguin cranium from Antarctica and its implications for body size diversity during the Eocene. Neues Jahrb. Geol. Palaeontol. Abh. 286, 229–233.
Houssaye, A., 2009. Pachyostosis" in aquatic amniotes: a review. Integr. Zool. 4, 325–340.
Ibañez, L., 2009. Anatomía de los surcos nasales y significado funcional de la glándula de la sal en aves marinas. Tesis de licenciatura, Univ. CAECE, Buenos Aires, Argentina.
Jadwiszczak, P., 2006. Eocene penguins of Seymour Island, Antarctica: the earliest record, taxonomic problems and some evolutionary considerations. Pol. Polar Res. 27, 287–302.
Jadwiszczak, P., 2012. Partial limb skeleton of a "giant penguin" Anthropornis from the Eocene of Antarctic Peninsula. Pol. Polar Res. 33, 259–274.
Ksepka, D.T., Bertelli, S., 2006. Fossil penguin (Aves: Sphenisciformes) cranial material from the Eocene of Seymour Island (Antarctica). Hist. Biol. 18, 389–395.
Ksepka, D.T., Clarke, J.A., 2010. The basal penguin (Aves: Sphenisciformes) *Perudyptes devriesi* and a phylogenetic evaluation of the penguin fossil record. Bull. Am. Mus. Nat. Hist. 337, 1–77.
Ksepka, D.T., Clarke, J.A., DeVries, T.J., Urbina, M., 2008. Osteology of *Icadyptes salasi*, a giant penguin from the Eocene of Peru. J. Anat. 213, 131–147.
Ksepka, D.T., Fordyce, R.E., Ando, T., Jones, C.M., 2012a. New fossil penguins (Aves, Sphenisciformes) from the Oligocene of New Zealand reveal the skeletal plan of stem penguins. J Vert. Paleontol. 32, 235–254.
Ksepka, D.T., Balanoff, S., Walsh, A., Revan, A., Ho, A., 2012b. Evolution of the brain and sensory organs in Sphenisciformes: new data from the stem penguin *Paraptenodytes antarcticus*. Zool. J. Linn. Soc. 166, 202–219.
Livezey, B.C., Zusi, R.L., 2006. Higher-order phylogenetics of modern Aves based on comparative anatomy: I. Methods and characters. Bull. Carn. Mus. Nat. Hist. 37, 1–544.
Marples, B.J., 1953. Fossil penguins from the mid-Tertiary of Seymour Island, Falklands Islands Dependencies. Surv. Sci. Rep. 5, 1–15.
Mayr, G., De Pietri, V.L., Love, L., Mannering, A.A., Scofield, R.P., 2017. A well-preserved new mid-Paleocene penguin (Aves, Sphenisciformes) from the Waipara Greensand in New Zealand. J. Vert. Paleontol. 37, e1398169.
Meister, W., 1962. Histological structure of the long bones of penguins. Anat. Rec. 43, 377–386.
Montes, M., Nozal, F., Santillana, S., Marenssi, S., Olivero, E., 2013. Mapa Geológico de la isla Marambio (Seymour) Escala 1: 20.000. Serie Cartográfica Geocientífica Antárctica.
Myrcha, A., Tatur, A., Del Valle, R., 1990. A new species of fossil penguin from Seymour Island. West Antarctica. Alcheringa 14, 195–205.
Myrcha, A., Jadwiszczak, P., Tambussi, C.P., Noriega, J.I., Gazdzicki, A., Tatur, A., Del Valle, R., 2002. Taxonomic revision of Eocene Antarctic penguins based on tarsometatarsal morphology. Pol. Polar Res. 23, 5–46.
Olson, S.L., 1985. The fossil record of birds. Avian Biol. 8, 79–238.
Paulina-Carabajal, A., Acosta Hospitaleche, C., Yury-Yáñez, R.E., 2015. Endocranial morphology of *Pygoscelis calderensis* (Aves, Spheniscidae) from the Neogene of Chile and remarks on brain morphology in modern Pygoscelis. Hist. Biol. 27, 571–582.
Proffitt, J.V., Clarke, J.A., Scofield, R.P., 2016. Novel insights into early neuroanatomical evolution in penguins from the oldest described penguin brain endocast. J. Anat. 229, 228–238.
Sadler, P.M., 1988. Geometry and stratification of Uppermost Cretaceous and Paleogene units on Seymour Island, northern Antarctic Peninsula. Geology and Paleontology of Seymour Island, Antarctic Peninsula. Geol. Soc. Am. Mem. 169, 303–320.
Sharpe, R.B.,1891. A review of recent attempts to classify birds. Proceedings of the Second International Ornithological Congress, 90. Budapest.
Slack, K.E., Jones, C.M., Ando, T., Harrison, G.L., Fordyce, R.E., Arnason, U., Penny, D., 2006. Early penguin fossils, plus mitochondrial genomes, calibrate avian evolution. Mol. Biol. Evol. 23, 1144–1155.
Snively, E., Russell, A.P., 2007a. Functional morphology of neck musculature in the Tyrannosauridae (Dinosauria, Theropoda) as determined via a hierarchical inferential approach. Zool. J. Linn. Soc. Lond. 151, 759–808.
Snively, E., Russell, A.P., 2007b. Functional variation of neck muscles and their relation to feeding style in Tyrannosauridae and other large theropod dinosaurs. Anat. Rec. 290, 934–957.
Stucchi, M., Urbina, M., Giraldo, A., 2003. Una nueva especie de Spheniscidae del Mioceno tardío de la Formación Pisco. Peru. Bull. Inst. Fr. Etud. Andin. 32, 361–375.
Tambussi, C.P., Degrange, F.J., Ksepka, D.T., 2015. Endocranial anatomy of Antarctic Eocene stem penguins: implications for sensory system evolution in Sphenisciformes (Aves). J. Vert. Paleontol. 35, e981635.
Walsh, S., Milner, A., 2011a. Evolution of the avian brain and senses. In: Dyke, G., Keiser, G. (Eds.), Living dinosaurs: the evolutionary history of modern birds. John Wiley and Sons, Ltd, West Sussex, pp. 282–305.
Walsh, S., Milner, A., 2011b. *Halcyornis toliapicus* (Aves: Lower Eocene, England) indicates advanced neuromorphology in Mesozoic Neornithes. J. Syst. Palaeontol. 9,173–181.
Wiley, D.F., Amenta, N., Alcantara, D.A., Ghosh, D., Kil, Y.J., Delson, E., Harcourt-Smith, W., Rohlf, F.J., St. John, K., Hamann, B., Motani, R., Frost, S., Rosenberger, A.L., Tallman, L., Disotell, T., O'Neill, R., 2007. Landmark Editor ver. 3.6. Institute for Data Analysis and Visualization (IDAV) and the University of California, Davis http://www.idav.ucdavis.edu/research/EvoMorph.

Wiman, C., 1905a. Über die alttertiären Vertebraten der Seymourinsel, 3. Wiss Ergeb Schwedischen Südpolar–Expd 1901–1903, pp. 1–37.
Wiman, C., 1905b. Vorläufige Mitteilung über die alttertiären Vertebraten der Seymourinsel. Bull. Geol. Inst. Uppsala. 6, 247–253.
Witmer, L.M., 1997. The evolution of the antorbital cavity of archosaurs: a study in soft-tissue reconstruction in the fossil record with an analysis of the function of pneumaticity. J. Vert. Paleontol. 17, 1–76.
Zusi, R.L., 1962. Structural adaptations of the head and neck in the Black Skimmer, *Rynchops nigra* Linnaeus. Publ. Nuttall Ornithol. Club. 3, 1–101.
Zusi, R.L., 1975. An interpretation of skull structure in the penguins. The biology of penguins., pp. 59–84.